

ZnO_xMgO_{1-x} (x=1.0, 0.70, 0.60, 0.20, 0.10) Nanostructures Thin Films

Ankita Sharma, Swati Arora

Department of Electronics and Communication Engineering, Swami Keshvanand Institute of Technology, Management & Gramothan, Jaipur, India

Email: anki.1988@yahoo.com, swati@skit.ac.in

Received 15.09.2022, received in revised form 02.10.2022, accepted 03.10.2022

DOI: 10.47904/IJSKIT.12.2.2028.31-34

Abstract: In this study it has been reported that composites of ZnO_xMgO_{1-x} were formed resting on ITO substrates with electron beam evaporation. Different MgO compositions, from zero to ninety percent doped, are expressed as atomic percentage success in doping MgO, as determined by XRD. It has been shown via research that the construction of a mesoporous structure is intimately associated to the tuning of the band gap as of 3.16 eV to 3.55 eV and the subsequent shifting of the transmission band edge by around 36 meV in the direction of higher energy. By analyzing UV-Vis Spectra, the Band Gap could be determined. Surface flaws have been shown to increase with MgO content, as confirmed by the investigation. Both undoped and doped Zn_{1-x}MgO_x thin films be deposit using an ultrasonic spray pyrolysis method over the substrate. Substitution of MgO ions for ZnO ions in the ZnO lattice is shown by a blue shift during the near-band-edge production and a transform in the lattice constant. Because of the structural transition from wurtzite (ZnO) to a combination of wurtzite and cubic (MgO) phases with greater Mg concentration (x C 0.21), a striking morphological transformation is seen. The FTIR analysis showed that the typical absorption peaks for Zn-O stretching mode were located at *442 cm⁻¹ and moved into the red area when the Mg level increased. One extra band about 523 cm⁻¹ was detected, most likely due to the Mg-related vibration mode in ZnO, in addition of the host phonons.

Keywords: Lattice parameters, E-Beam Deposition, transmission band edge, mesoporous, defect

1. INTRODUCTION

Researchers have recently been focusing on Nano crystalline thin film production and characterization. This thin film technique has captivated researchers in the disciplines of optics, microelectronics, and nanotechnology. The literature suggests that thin film has emerged as a subject of interest for academics throughout the world in the last several years. This convergence of global interest and scholarly investigation into the issue at hand was the main draw for this sector. As a wonderful material for use in light-emitting devices and displays, zinc oxide's

luminescence is an essential feature. To increase the band gap of ZnO, several researchers have tried synthesizing its solid solution with magnesium oxide. The current research aims to investigate and report on the characteristics properties of compound (ZnO)_x-(MgO)_{1-x} thin films created using the E-beam physical vapor deposition process. The semiconductor properties of (ZnO)_x-(MgO)_{1-x} allow for a thick range of possible uses. The goal of this study is to determine how the addition of magnesium to (ZnO)_x-(MgO)_{1-x} films produced using the E-beam physical vapour deposition ZnO is often used. The performance of the device may be best understood in terms of its absorbency, or how much light it can take in, and the size of its grains. Alternatively, magnesium atoms may replace zinc atoms in ZnO to increase the band gap. A wide range of deposition methods, as well all been put to use in this particular region. Widespread attention has been paid to both single-layer and multilayer deposition of semiconductor thin films for use in real-world devices. These thin films have evolved over time to combine the useful qualities of two distinct materials, and in some instances hey have delivered better or otherwise novel physical properties.

2. EXPERIMENTAL

ZnO_xMgO_{1-x}(x=1.0, 0.70, 0.60, 0.20, 0.10) have been made-up throughout E-beam deposition method. At room temperature, (ZnO)_x-(MgO)_{1-x} with varying Zn contents were formed using ultrasonic pulse deposition. When looking for zinc and magnesium, two different aqueous solutions were selected: Zn(CH₃COO)₂.2H₂O (AR) and Mg(CH₃COO)₂.4H₂O (AR), respectively. The following quantities of solution were used to produce (ZnO)_x-(MgO)_{1-x} films with varying Zn concentrations (0 B x B 0.3): Zinc acetate, 0.01 M; deionized water, 50 ml (resistivity = 18.2 MX cm); methanol, 20 ml (Merck 99.5%); ethanol, 30 ml (Merck 99.5%); acetic acid, 30 ml (Merck 99.5%); magnesium acetate, 10-30%

(Mg, at.%). To avoid the development of hydroxides, the pH of aqueous solutions was lowered by adding a little quantity of acetic acid, bringing it to about 4.8. The most readily available oxidizer is water. Since rapid conversion of the precursor mist into vapour form is a crucial factor in achieving high-quality films, the use of volatile solvents like methanol and ethanol was a no-brainer. This study makes use of a commercial ultrasonic atomizer (VCX 134 AT) and a heated substrate holder for ultrasonic spraying. In this case, the ultrasonic vibrator operated at a occurrence of 40 kHz and a influence input of 130 W was used. At 40 kHz, the typical drop size is 45 l throughout the deposition; we maintained a stable solution flow rate of 0.1 ml/min and a nozzle-to-substrate distance of 5 cm. At 450 C, $(\text{ZnO})_x-(\text{MgO})_{1-x}$ thin films were formed onto microscope cover glass substrates (30 9 12 9 1.2 mm³). It took around half an hour to an hour and a half to deposit the money. A thermocouple was used to measure and electrically regulate the substrate's temperature.

3. RESULTS AND DISCUSSIONS

3.1. Structural Study

The peaks of diffraction are hexagonal for ZnO and cubic for MgO are indexed using JCPDS card No. 80-0075 and 78-0430[6]. Figure 1 displays XRD diagrams for $\text{ZnO}_x\text{MgO}_{1-x}$ ($x=1.0, 0.70, 0.60, 0.20, 0.10$) composite. The spiky peaks with regular allocation indicate the incidence of ZnO (wurtzite structure)[7] and MgO(The pattern is indexed using the crystal structures of ZnO-MgO, which are respectively hexagonal and cubic. ZnO peaks are present, as well as the (111) and (200) peaks, indicating composite production [8]. The relative

strengths of the (111) and (200) peaks both increased with increasing MgO content.

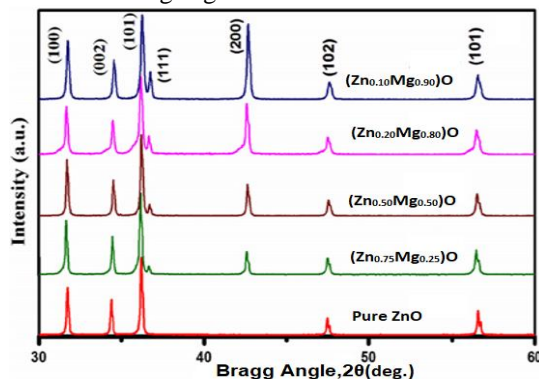


Fig 1: MgO in $(\text{Zn}_x\text{Mg}_{1-x})\text{O}$ composites X-Ray Diffraction Patterns

3.2. Morphological Properties

SEM of $\text{ZnO}_x\text{MgO}_{1-x}$ composites (Fig. 2) reveal certain nanostructured grains with a hexagonal crystalline shape that are uniformly distributed throughout the material. These SEM pictures show the effect that increasing the Mg doping level has on the ZnO surface [8]. All the samples have uneven, grainy surfaces covered with nano tubes of varying sizes and shapes. These crystals are scattered and confused in an unorganized fashion. Granule size was observed to decrease from 109 nm to 55 nm at what time the MgO content x was adjusted from 0 to 50% (Fig. 2(a) and (b)) (c). High-doped ZnO samples, as shown in Fig. 2(d), have a lower grain density and more coalescence of tiny grains, as shown in [9]. Grain boundaries and big grains that are partially obscured by smaller crystallites may be seen in Fig. 1(e).

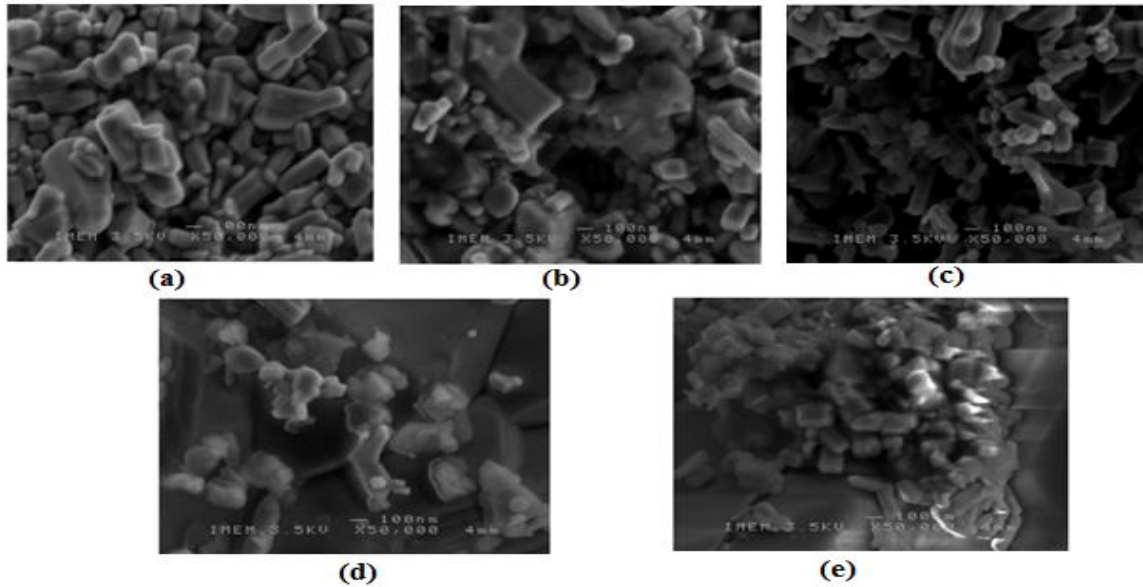


Figure 2: SEM images obtained for composites: (a) Pure ZnO (b)(Zn_{0.70}Mg_{0.30})O (c)(Zn_{0.60}Mg_{0.40})O (d)(Zn_{0.20}Mg_{0.80})O (e)(Zn_{0.10}Mg_{0.90})O

3.3. Optical Properties

Tauc scheme is use to determine the optical band gap of ZnO_xMgO_{1-x} (x=1.0, 0.70, 0.60, 0.20, 0.10) composite on substrate. The linear zone is shown in the figure of (hν)² against photon energy right above the optical absorption edge [10-13]. This direct band gap is connected to the photon energy-absorption coefficient (h) plot by the following relation [14]: αhν = K. (hν - E_g)² Absorption coefficient and photon energy (h) are substituted for K, which is a constant. Optical absorption measurements of (hν)² vs h are shown in Fig. 3 (Tauc Plot). We find that when MgO concentration increases, so does the band gap. Figure 3 depicts the shift in optical band gap for ZnO_xMgO_{1-x} for composites (x=1.0, 0.70, 0.60, 0.20, 0.10) with varying MgO concentration. E_g is determined to have values of 3.16, 3.22, 3.27, 3.34, and 3.55 eV as the concentration is varied from x=1.00 to x=0.10. There are two possible

explanations for the blue shift in the band gap that has been observed. Size-dependent quantum effect I (2) Shifts in the electrical structure. [15-17]

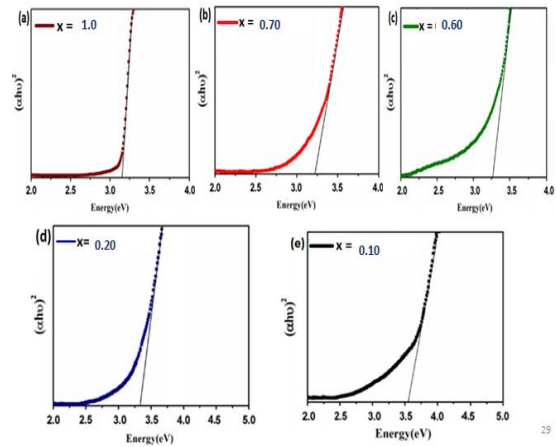


Figure 3: (αhν)² versus hν plot of (Zn_xMg_(1-x))O composites

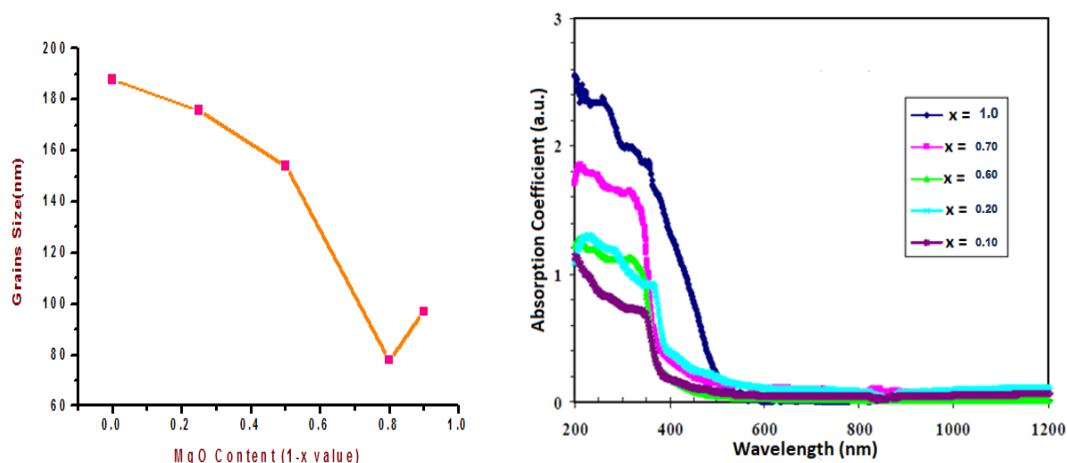


Figure 3: $(\alpha h\nu)^2$ versus $h\nu$ plot and Absorption Coefficient Spectra of $(\text{Zn}_x\text{Mg}_{1-x})\text{O}$ composites: (a) $x=1.0$ (b) $x=0.70$ (c) $x=0.60$ (d) $x=0.20$ (e) $x=0.10$

ZnO Content(x)	1	0.70	0.60	0.20	0.10
MgO Content (1-x Value)	0	0.30	0.40	0.80	0.90
Grain Size (nm)	188	176	154	78	97

4. CONCLUSION

Thin films composed of $\text{ZnO}_x\text{-MgO}(1-x)$ are produced using an electron beam deposition method. The XRD analysis demonstrates the composite's genesis. As the SEM image demonstrates, the materials are porous. Similarly, it reveals the rougher surfaces of the samples coated with granules of prismatic forms and varying sizes. The size of the crystallites has been shown to grow with Mg concentration by FESEM analysis. As the MgO concentration rises, the band gap be effectively adjusted commencement 3.16 to 3.55 eV.

REFERENCES

- [1] G. Decher, J. B. Schlenoff, "Multilayer Thin Films: Sequential Assembly of Nanocomposite Materials", Wiley-2 nd Ed, 2012.
- [2] Catherine Picart, Frank Caruso, Jean-Claude Voegel, Gero Decher, "Layer-by-Layer Films for Biomedical Applications", Wiley-VCH, 2003
- [3] Y. S. Lim, J. S. Jeong, J. Bang, J. Kim "CaO buffer layer for the growth of ZnO thin film", Journal of Solid-State Communications, vol. 150, 2010, pp. 428- 430.
- [4] Yan Xu, Jingjie Jin, Xianliang Li, Yide Han, Hao Meng, Tianyu Wang, Xia Zhang, "Simple synthesis of ZnO nanoflowers and its photocatalytic performances toward the photodegradation of metamitron", Materials Research Bulletin, vol. 76, 2016, pp. 235-239.
- [5] Liqing Liu, Kunquan Hong, Xing Ge, Dongmei Liu, Mingxiang Xu, "Controllable and Rapid Synthesis of Long ZnO Nanowire Arrays for Dyesensitized Solar Cells", J. Phys. Chem. C, vol. 118, 2014, pp. 15551–15555.
- [6] Laurent Schlur, Anne Carton, Patrick L  v  que, Daniel Guillon, Genevi  ve Pourroy "Optimization of a New ZnO Nanorods Hydrothermal Synthesis Method for Solid State Dye Sensitized Solar Cells Applications", J. Phys. Chem. C, 117, 2013, pp. 2993–3001.
- [7] K. Koike, T. Aoki, R. Fujimoto, S. Sasa, M. Yano, S. Gonda, R. Ishigami, K. Kume, "Radiation hardness of single-crystalline zinc oxide films" J. Phys. Status Solidi C, vol. 9, 2012, pp.1577–1579.
- [8] Shashikant Sharma, Bernhard C. Bayer; Viera Skakalova; Ghanshyam Singh, Chinnamuthan Periasamy, "Structural, Electrical, and UV Detection Properties of ZnO/Si Heterojunction Diodes" IEEE Transactions on Electron Devices, vol. 63, 2016, pp.1949-1956.
- [9] R. Pietruszka. B. S. Witkowski, P. Caban, E. Zielony, K. Gwozdz, P. Bieganski, E. Placzek Popko, "New efficient solar cell structures based on zinc oxide nanorods Solar Energy Materials and Solar Cells", Journal of Solar Energy Materials and Solar Cells, vol. 143, 2015, pp. 99-104.12. T. Minemoto, T. Negami, S. Nishiwak, Thin Solid Films, 372 (2000) 173.